





Article

Easy and Efficient Recovery of EMIMCl from Cellulose Solutions by Addition of Acetic Acid and the Transition from the Original Ionic Liquid to an Eutectic Mixture

Huan Zhang ¹, Andreea Ionita ¹, Pilar F. Serriñan ¹, María Luisa Ferrer ^{1,*}, María A. Rodríguez ², Aitana Tamayo ³, Fausto Rubio Alons ³, Francisco del Monte ¹ and María C. Gutiérrez ^{1,*}

¹ Instituto de Ciencia de Materiales de Madrid-ICMM, Consejo Superior de Investigaciones Científicas-CSIC, Campus de Cantoblanco, 28049 Madrid, Spain; huanzhang0107@163.com (H.Z.); andreeai@ucm.es (A.I.); pilar.serinan@csic.es (P.F.S.); delmonte@icmm.csic.es (F.d.M.)

² Area de Cristalografía y Mineralogía, Facultad de Ciencias, Universidad de Extremadura, 06006 Badajoz, Spain; marodgon@unex.es

³ Instituto de Cerámica y Vidrio-ICV, Consejo Superior de Investigaciones Científicas-CSIC, Campus de Cantoblanco, 28049 Madrid, Spain; aitanath@icv.csic.es (A.T.); frubio@icv.csic.es (F.R.A.)

* Correspondence: mferrer@icmm.csic.es (M.L.F.); mcgutierrez@icmm.csic.es (M.C.G.)

Abstract: Ionic liquids (ILs) and deep eutectic solvents (DESs) are the two most widely used neoteric solvents. Recently, our group described how the simple addition of acetic acid (AcOH) to 1-Ethyl-3-methylimidazolium chloride (EMIMCl) could promote the transition from the original IL to an eutectic mixture of EMIMCl and AcOH. Herein, we studied how cellulose regeneration and EMIMCl recovery from EMIMCl solutions of cellulose could be benefited by the significant differences existing between EMIMCl- and EMIMCl·AcOH-based mixtures and the easy switching from one to the other. Finally, we also demonstrated that the transition could also be accomplished by addition of acetic anhydride and water so that the process could be eventually useful for the achievement of highly acetylated cellulose.

Keywords: ionic liquids; deep eutectic solvents; cellulose dissolution; cellulose regeneration; ionic liquid recovery; cellulose acetylation



Citation: Zhang, H.; Ionita, A.; Serriñan, P.F.; Ferrer, M.L.; Rodríguez, M.A.; Tamayo, A.; Rubio Alons, F.; del Monte, F.; Gutiérrez, M.C. Easy and Efficient Recovery of EMIMCl from Cellulose Solutions by Addition of Acetic Acid and the Transition from the Original Ionic Liquid to an Eutectic Mixture. *Molecules* **2022**, *27*, 987. <https://doi.org/10.3390/molecules27030987>

Academic Editor: Rafał M. Lukasiak

Received: 30 December 2021

Accepted: 24 January 2022

Published: 1 February 2022

Publisher's Note: MDPI stays neutral with regard to jurisdictional claims in published maps and institutional affiliations.



Copyright: © 2022 by the authors. Licensee MDPI, Basel, Switzerland. This article is an open access article distributed under the terms and conditions of the Creative Commons Attribution (CC BY) license (<https://creativecommons.org/licenses/by/4.0/>).

1. Introduction

Both ionic liquids (ILs) and deep eutectic solvents (DESs) have become the two most popular neoteric solvents. ILs were originally conceived as molten salts combining a single organic cation and a single organic or inorganic anion so that the charges are neutralized [1]. More recently, certain mixtures of ILs have resulted in the formation of “new solutions” with properties that were somehow different from those of the original ILs [2]. DESs were first described by Abbot and coworkers in 2003 [3] as supramolecular complexes formed between one hydrogen bond donor—HBD—and one hydrogen bond acceptor—HBA, typically an ammonium or phosphonium salt—with the charge delocalization that occurs between the HBD and the HBA being responsible of the decrease in the melting point of the mixture as compared with those of its individual components.

Along the subsequent years of ILs and DESs discovery, few attempts were made to correlate DESs and ILs [4]. More recently, this view has changed thanks to studies describing the presence of H bonds in ILs and aqueous dilutions of ILs with the anion (chloride in most of cases, but other ones may be too) playing a critical role [5–10], similarly to what happens in DESs and DESs dilutions [11–15]. In fact, aqueous dilutions of hydrated salts at a certain range of dilution have also been recently described as DESs [16]. Moreover, recent works have described the preparation of mixtures of 1-Ethyl-3-methylimidazolium chloride (EMIMCl, playing the role of HBA) and succinonitrile [17], several amides [18,19] and glycol-derivatives [20–22], and differentazole [23–25] and pyridinium [26] bases, playing

the role of HBDs. Most of these DESs, as well as some others based on different imidazolium salts such as 1-butyl-3-methylimidazolium chloride and bromide (BMIMCl and BMIMBr), or 1-hexyl-3-methylimidazolium chloride (HMIMCl [17,27]), were used for gas absorption (mainly SO₂, but also CO₂ or NH₃), and insights about the HB complex structure were obtained by NMR and FTIR spectroscopies as well as by theoretical calculations. In addition, very recent studies performed in our group by NMR spectroscopy and molecular dynamics simulations provided a more detailed description of the HBs formed between EMIMCl and acetic acid (AcOH as the HBD) that allowed one eutectic mixture to be achieved [28]. Interestingly, this work also suggested the possibility of forming this sort of eutectic mixture with different acids as the HBDs (e.g., formic and octanoic acids) as well as with different EMIM-based ILs (e.g., EMIMTFSI).

Herein, we study how the stoichiometric addition of AcOH to a EMIMCl solution of cellulose allows an easy and efficient recovery of EMIMCl thanks to the different solvent properties of EMIMCl- and EMIMCl·AcOH-based mixtures resulting after AcOH addition. Moreover, we design a process to obtain acetylated cellulose in which the transition from EMIMCl- and EMIMCl·AcOH-based mixtures was promoted by addition an efficient acetylation agent such as acetic anhydride (Ac₂O) instead of the above-mentioned AcOH. The study of EMIMCl recovery and cellulose regeneration either in the non-acetylated or acetylated form was performed by FTIR and NMR spectroscopy.

2. Results and Discussion

Based on the specific physicochemical features described elsewhere for EMIMCl- and EMIMCl·AcOH-based mixtures [28], their solvent properties should also be different. There are many papers on dissolving cellulose in the ionic liquid 1-ethyl-3-methylimidazolium acetate (EMIMOAc), which is a very good cellulose solvent (>20 wt% at 80 °C) [29,30]. Moreover, it is well known EMIMCl is an excellent solvent for cellulose [31]. Recent works using molecular dynamics simulations revealed the critical role played by the chloride anion that penetrates between cellulose molecular chains and forms hydrogen bonds with them [32]. The replacement of the original hydrogen bonds between chains promotes their cleavage and ultimately results in cellulose dissolution. Besides the solvent capability, the subsequent cellulose coagulation and IL recovery also accounts on the greenness and economic viability of an IL process for biomass processing. Anti-solvents such as water, ethanol, methanol, acetone, acetonitrile, etc., have been widely used for this purpose, as in the seminal work by Swatloski et al., first describing the cellulose dissolution in ILs [33,34]. Among these solvents, water is chosen in most cases because it is safe, environmentally benign, and inexpensive. However, as regeneration of cellulose occurs when contacting the cellulose solution with the aqueous coagulation bath, the polymer profile at the point of precipitation exhibits a very high interfacial concentration, thus favoring the formation of a dense polymer “skin”, through which further coagulant has to diffuse for bulk sample precipitation. Considering also the competition between the water–anion, cellulose–anion, cellulose–water, cellulose–cation, and anion–cation interactions, full IL separation from cellulose typically requires more than one washing cycle. Based on this, recovering IL for reuse is currently energy intensive—e.g., first involving extensive washing steps with water to recover the IL entrapped within the regenerated cellulose and then intensive evaporative steps for separating the water from the IL—and ultimately compromises the greenness of the whole process. Thus, as stated in a recent review on this field, the development of more efficient and energy-saving methods for the recycling of ILs is required [35].

Interestingly, where both EMIMCl and EMIMOAc are excellent solvents for cellulose dissolution [32,36,37], cellulose solubility is negligible in EMIMCl·AcOH-based mixtures, most likely because the strong participation of chloride anions in H bond complexes forming the DES makes them basically unavailable to form new H bonds with cellulose chains. Thus, we hypothesized a process for cellulose regeneration where, after cellulose dissolution in EMIMCl, transition from EMIMCl to EMIMCl·AcOH upon addition of

AcOH would result in cellulose precipitation and separation from the EMIMCl liquid phase, without the addition of any antisolvent.

For comparison, we first performed cellulose regeneration using bare water as the anti-solvent (see entries #1 and #2 in Table 1). In this case, cellulose was precipitated by H₂O addition (e.g., 10 mL) and gentle stirring over 2 h. The experiment was carried out at 2 different temperatures (e.g., 20 and 4 °C) and on 2 different EMIMCl solutions (e.g., with cellulose contents of 2 and 8 wt%). After centrifugation, cellulose was concentrated at the bottom of the centrifuge tube and separated from the supernatant. The precipitate was subsequently washed with further H₂O (e.g., 10 mL), centrifuged, and separated from the supernatant, and this process repeated 3 more times (e.g., 10 mL in each) for a total of 5 washing cycles, following a similar process to those described previously [38,39]. Cellulose recovery was accomplished by simple drying of remaining H₂O, while EMIMCl recovery was accomplished by submission of the supernatant aqueous phase to a freeze-drying process. When H₂O addition and washing was carried out at 20 °C, cellulose recovered as precipitate was quite poor (ca. 80%). Actually, this poor recovery was anticipated by the cloudy aspect of the supernatant phase (Figure 1), that revealed the presence of some cellulose yet dispersed in the liquid phase. Data of EMIMCl recovery shown in Table 1 (entry #2) should be taken with caution as the presence of cellulose in the supernatant phase resulted in the ultimate overestimation of any figure coming from this experiment. Cellulose recoveries above 95% (near full recoveries, within the experimental error) were obtained when the process was carried at 4 °C and we obtained a fully transparent supernatant phase (Figure 1). EMIMCl recovery was ca. 71% after the 1st washing cycle and we needed 4 additional washing cycles (and the freeze-drying of the supernatant phases, that is, ca. 50 mL) to basically get full EMIMCl recovery (ca. 98%).

Table 1. Data of recovered EMIMCl after cellulose precipitation from EMIMCl dilutions with 2 and 8 wt% cellulose contents.

Entry	Cellulose Content in Dilution (wt%)	Antisolvent	Recovered EMIMCl (%)		
			After AcOH Addition	After First H ₂ O Addition	After End of Washing Cycles
#1	2	H ₂ O (10 mL) at 4–5 °C	–	71 ^b	97.8 ^c
#2	2	H ₂ O (10 mL) at 20 °C	–	71 ^b	90.0 ^c
#3	2	AcOH (10 mL) at 20 °C	62.3 ^a	91.2 (62.3 ^a + 28.9 ^b)	99.6 ^d
#4	2	AcOH (10 mL) at 60 °C	63.3 ^a	92.6 (63.3 ^a + 29.3 ^b)	99.6 ^d
#5	2	AcOH (1 equivalent) at 60 °C	32.4 ^a	90.6 (32.4 ^a + 58.2 ^b)	99.1 ^d
#6	2	AcOH (3 equivalents) at 60 °C	42.8 ^a	90.2 (42.8 ^a + 47.4 ^b)	98.2 ^d
#7	8	AcOH (10 mL) at 20 °C	24.9 ^a	88.8 (24.9 ^a + 63.9 ^b)	98.6 ^d
#8	8	AcOH (10 mL) at 60 °C	41.5 ^a	88.2 (41.5 ^a + 46.7 ^b)	99.8 ^d
#9	8	AcOH (1 equivalent) at 60 °C	6.8 ^a	85.5 (6.8 ^a + 78.7 ^b)	99.1 ^d
#10	8	AcOH (3 equivalents) at 60 °C	19.3 ^a	89.3 (19.3 ^a + 70.0 ^b)	99.0 ^d

^a EMIMCl recovered after AcOH removal by thermal treatment at 60 °C under air flow; ^b EMIMCl recovered after H₂O removal by freeze-drying; ^c EMIMCl recovered after 4 additional washing cycles; ^d EMIMCl recovered after 2 additional washing cycles.

Based on the possibility for transitioning from EMIMCl- to EMIMCl·AcOH-based mixtures upon addition of AcOH and the negligible cellulose dissolution in these latter mixtures, we slightly modified the cellulose regeneration process trying to avoid or at least reduce the use of H₂O for cellulose precipitation and separation from the EMIMCl liquid phase. Thus, we added AcOH (e.g., 10 mL) to the EMIMCl solution of cellulose so that cellulose precipitated upon the transition from EMIMCl- to EMIMCl·AcOH-based mixtures. The clear aspect of the supernatant phase obtained in this case (Figure 1) anticipated an excellent cellulose recovery (e.g., ca. 100%), regardless of whether the process was carried out at 20 °C. Meanwhile, the boiling point of AcOH (ca. 118 °C) allowed its removal from EMIMCl·AcOH-based mixtures by thermal treatment at 60 °C under air flow (Figure S1). Thus, the application of this treatment to the supernatant resulted in AcOH evaporation and an EMIMCl recovery above 60% (Table 1). Interestingly, AcOH could also be added stoichiometrically (e.g., 1, 2, or 3 equivalents to obtain EMIMCl·1HOAc, EMIMCl·2HOAc, or EMIMCl·3HOAc, respectively). In these cases, the process was carried out at 60 °C to decrease the viscosity of the mixture and allow for a better homogenization. Differences in the amount of recovered EMIMCl coming from first precipitation upon the use of different temperatures, amount of AcOH (e.g., 1, 2, or 3 equivalents, or 10 mL) and cellulose contents in solution (e.g., 2 or 8 wt%) indeed confirmed the role played by viscosity in the recovery process (Table 1). The process continued washing the precipitated cellulose with successive additions of H₂O. Interestingly, EMIMCl recovery increased to ca. 90% after the 1st washing cycle (e.g., with 10 mL), largely improving the recovery yield obtained without the aid of EMIMCl- to EMIMCl·AcOH-based DESs transition (ca. 71%). Full EMIMCl recovery (ca. 99%) was obtained with only two additional washing cycles (Table 1).



Figure 1. Picture of the supernatant phase obtained after addition of H₂O at 20 °C (1), H₂O at 4–5 °C (2), or AcOH at either 20 or 60 °C (3) to EMIMCl solutions with 2 wt% (left) and 8 wt% (right) cellulose contents.

¹H NMR spectra of recovered EMIMCl (from both processes, without or with the aid of AcOH addition) exhibited the same peaks than the original EMIMCl (Figure 2). The efficient recovery of EMIMCl in its original form open the path to its reuse in subsequent treatment processes, thus helping to make the process economically viable. Meanwhile, regenerated cellulose was characterized by X-ray diffraction (XRD), Raman and FTIR spectroscopy, and thermogravimetric analysis (TGA). Cellulose regeneration from solution typically implies a crystalline transition from its native lattice (cellulose I) to the more thermally stable cellulose II lattice [40]. In our case, regenerated cellulose was amorphous, as revealed by the vanishing in XRD pattern of any crystalline diffraction peak characteristic of microcrystalline cellulose (MCC) and the appearance of a broad scattering peak

centered at ca. 30° in 2θ (Figure S2) [41]. Raman spectra of regenerated cellulose showed bands at 380 cm^{-1} assigned to the out of plane breathing of glucose ring, at 896 cm^{-1} assigned to glucose ring deformation, at $1090\text{--}1120$ and 1160 cm^{-1} assigned to skeletal deformation, at 1315 and $1338\text{--}1378\text{ cm}^{-1}$ assigned to C–C–H, C–O–H, and O–C–H bendings, and at 1470 cm^{-1} assigned to CH_2 bending (Figure S3) [42]. Interestingly, the main difference between regenerated cellulose and the original MCC was in the bands at 380 and 1096 cm^{-1} , typically used to determine the cellulose crystallinity [43]. As for recovered EMIMCl, no significant differences were observed between celluloses recovered without or with AcOH addition. Actually, differences in the regenerated cellulose obtained by the use of one process or the other were only observed by FTIR spectroscopy (Figures 3 and S4). In both cases, FTIR spectra exhibited the typical bands of MCC at $3337\text{--}3362\text{ cm}^{-1}$ assigned to OH stretching, at $2891\text{--}2896\text{ cm}^{-1}$ assigned to CH stretching, at 1430 cm^{-1} assigned to CH_2 deformation, at $1370\text{--}1315\text{ cm}^{-1}$ assigned to C–H and O–H deformation cm^{-1} , and at 1045 cm^{-1} assigned to C–O–C pyranose ring skeletal vibration, among the most significant [44,45]. However, the FTIR spectra of regenerated cellulose obtained after addition of AcOH exhibited a band at 1742 cm^{-1} of low intensity that revealed the occurrence of partial cellulose acetylation [46,47]. The low degree of substitution (DS) was further confirmed by the insolubility of our partially acetylated cellulose in DMSO, CH_3Cl , or acetone, these are typical solvents used to measure the DS by NMR spectroscopy [46,47]. Interestingly, this partial acetylation resulted in an enhancement of the thermal stability of cellulose regenerated with AcOH, as compared with that regenerated without AcOH (see TGA in Figure S5).

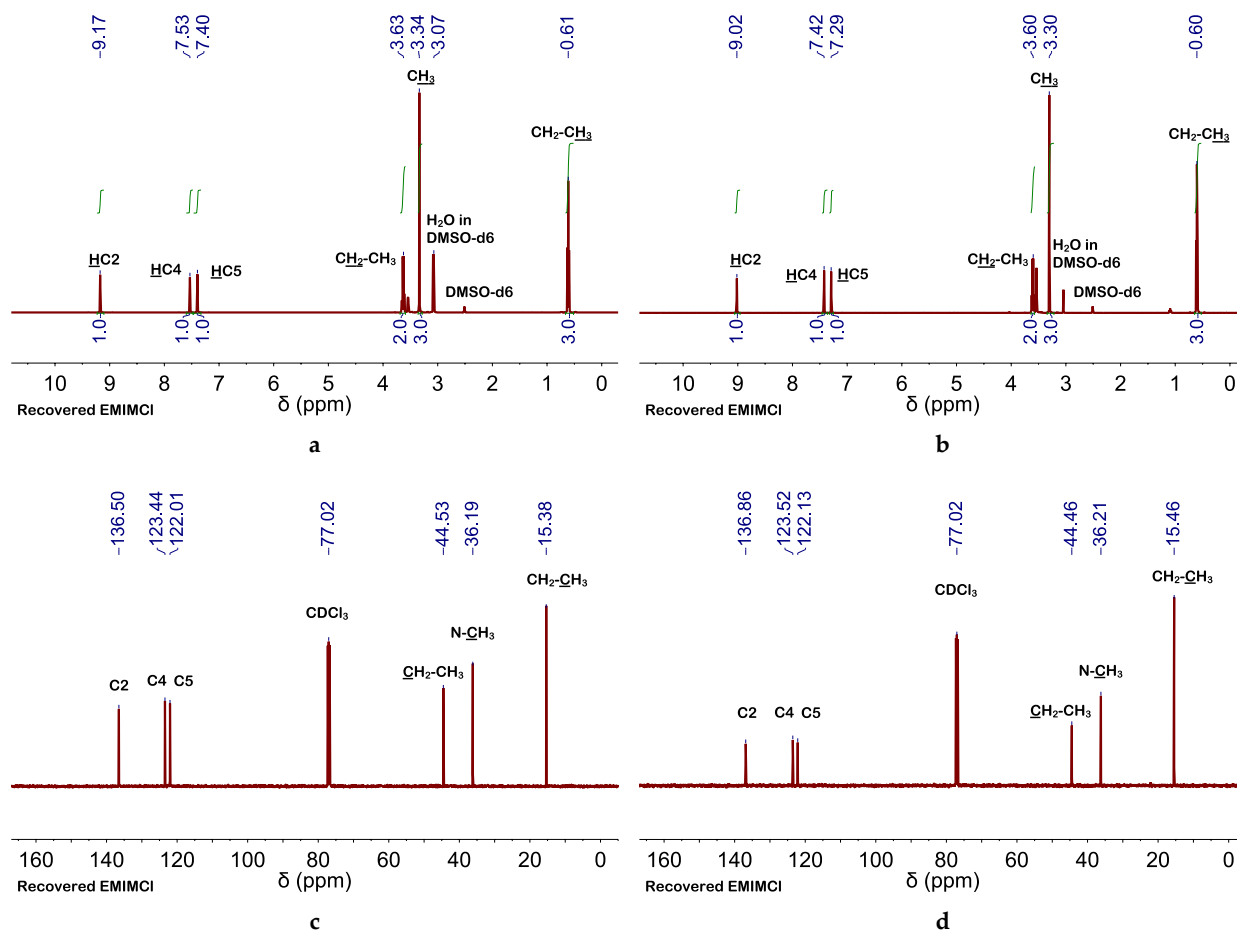


Figure 2. (a,b) ^1H and (c,d) ^{13}C NMR spectra of recovered EMIMCl (a,c) using H_2O as the antisolvent or (b,d) adding first AcOH and promoting the transition from EMIMCl- to EMIMCl·HOAc-based mixtures. ^1H and ^{13}C NMR spectra were performed at 85 and 25°C , respectively.

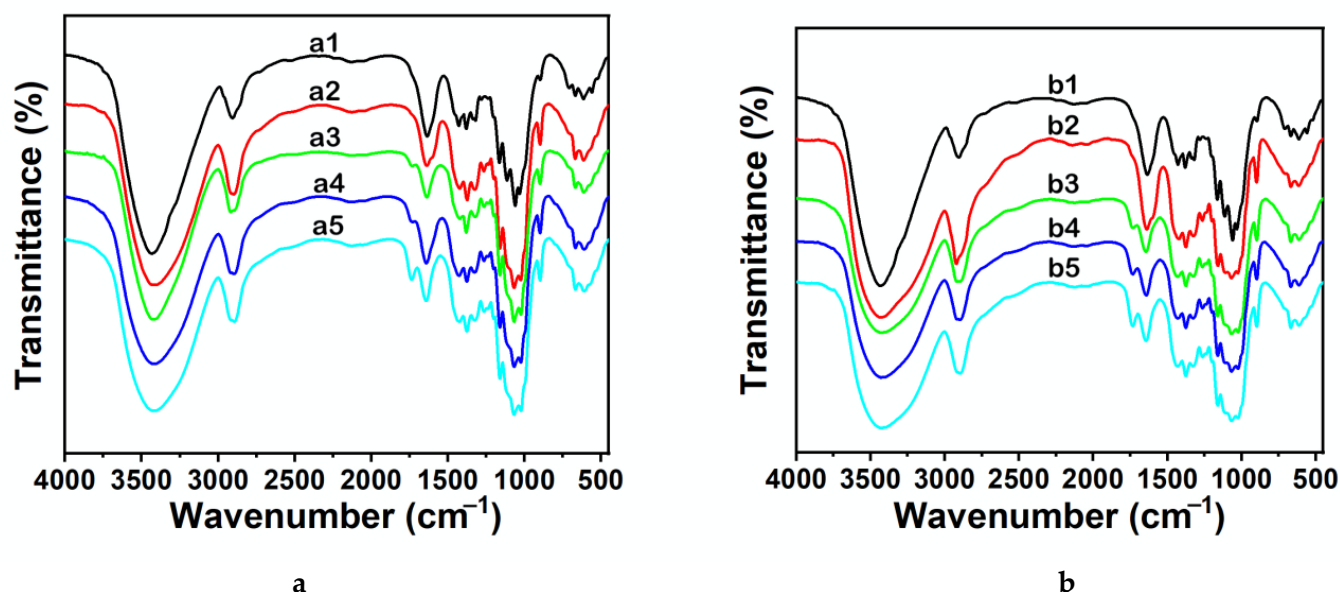


Figure 3. FTIR spectra of cellulose regenerated from EMIMCl solutions. The cellulose contents were 2 wt% (a) and 8 wt% (b). The antisolvent used for cellulose precipitation was either water (10 mL) at 20 °C (a2, b2, red line) or 1 equivalent of AcOH (a3, b3, green line), 2 equivalents of AcOH (a4, b4, blue line), or 3 equivalents of AcOH (a5, b5, light blue line) at 60 °C. The spectrum of MCC was included in both graphics for comparison (a1, b1, black line).

The occurrence of cellulose acetylation in EMIMCl and EMIMOAc solutions of cellulose has been widely described and high DSs were found with the use of high temperatures (e.g., ca. 100 °C), acid catalysis, and/or acetylating agents (e.g., vinyl acetate, acetic anhydride (Ac₂O), etc.) [39,48–53]. Among these options, we explored two that could be adapted to our process. First one was adding Amberlyst (e.g., a solid acid catalyst that could be separated from the reaction medium by simple filtration) [49] besides AcOH to the EMIMCl solution of cellulose. The presence of Amberlyst favored cellulose acetylation, more so than without using Amberlyst, as revealed by the high intensity of the band at 1742 cm⁻¹ (see FTIR spectra in Figure S6), as well as the increase in the thermal stability (see TGA curve in Figure S7). The second option consisted of the Ac₂O (instead of AcOH) addition to the EMIMCl solution of cellulose. As mentioned above, Ac₂O is an effective acetylation agent [52,53]. Moreover, transitioning from EMIMCl- to EMIMCl·AcOH-based DESs could also be accomplished in the presence of H₂O by Ac₂O hydrolysis (Figure 4). Cellulose acetylation occurred quite efficiently (even more than when using Amberlyst) as revealed by the intensity of the bands at 1742 cm⁻¹ in the FTIR spectra, depicted in Figure 5, as well as the DS (e.g., of ca. 2.5, 2.9, and 3 for acetylation with 0.5, 1, and 1.5 equivalents of Ac₂O, respectively) obtained by NMR spectroscopy (Figures 6 and S8), as described elsewhere [54]. TGA curves also revealed the increase in the thermal stability of the acetylated cellulose (Figure S9). Interestingly, cellulose and EMIMCl recoveries were as good as those obtained with AcOH (e.g., in terms of both yields and purity of recovered EMIMCl, see Figure S10).

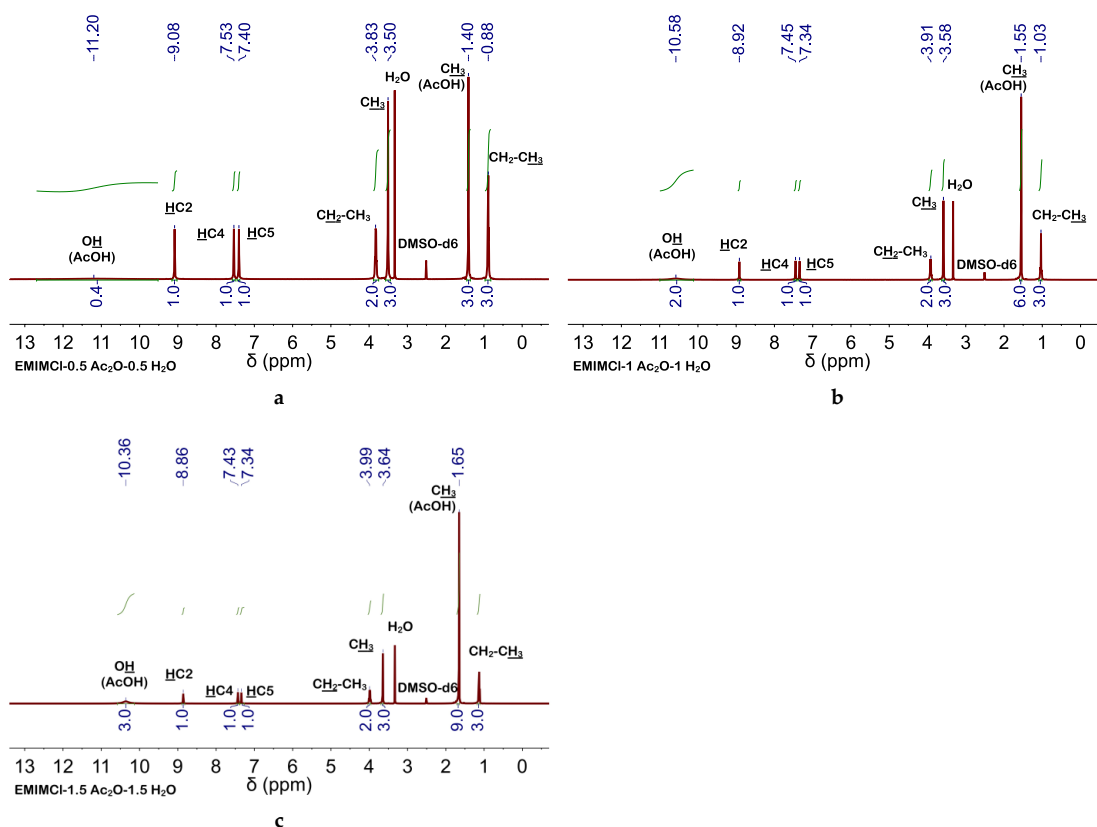


Figure 4. ^1H NMR spectra of EMIMCl-HOAc-based DESs; (a) EMIMCl-1HOAc obtained by addition of 0.5 equivalents of Ac₂O and 0.5 equivalents of H₂O to 1 equivalent of EMIMCl, (b) EMIMCl-2HOAc obtained by addition of 1 equivalent of Ac₂O and 1 equivalent of H₂O to 1 equivalent of EMIMCl, and (c) EMIMCl-3HOAc obtained by addition of 1.5 equivalents of Ac₂O and 1.5 equivalents of H₂O to 1 equivalent of EMIMCl. All ^1H NMR spectra were performed at 25 °C.

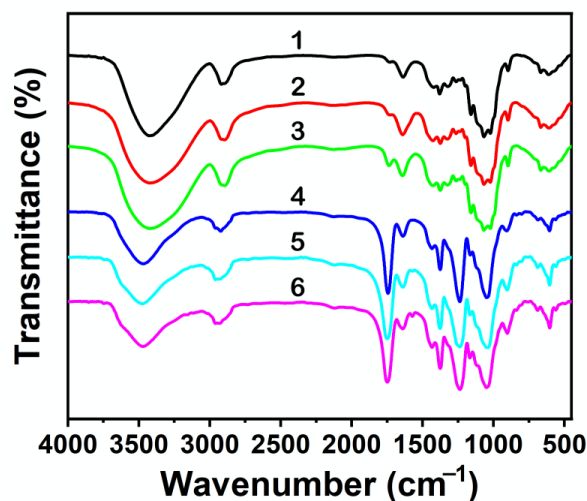


Figure 5. FTIR spectra of cellulose regenerated from EMIMCl solutions with 2 wt% cellulose content. Acetylation was carried out at 60 °C in the presence of 0.5 equivalent of Ac₂O (4, dark blue line), 1 equivalent of Ac₂O (5, light blue line), or 1.5 equivalents of Ac₂O (6, pink line), followed by the addition of 10 mL of H₂O to promote the EMIMCl- to EMIMCl-HOAc-based DESs transition and cellulose precipitation. The FTIR spectra of precipitated cellulose obtained upon the addition at 60 °C of 1 equivalent of AcOH (1, black line), 2 equivalents of AcOH (2, red line), or 3 equivalents of AcOH (3, green line) were also included for comparison.

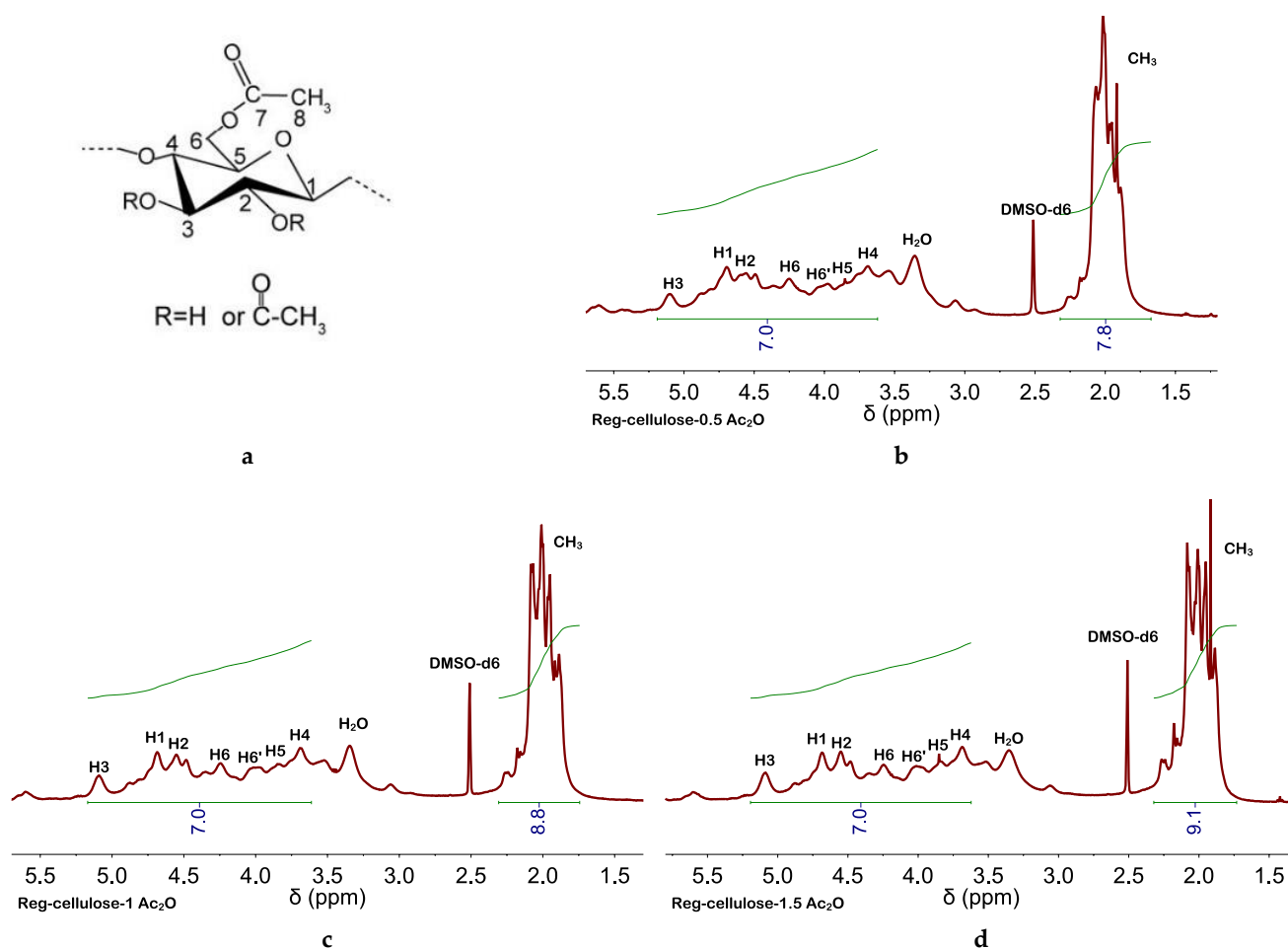


Figure 6. Glucose unit with labelled atoms (a) used for the assignment of peaks in the ^1H NMR spectra of cellulose obtained after acetylation at 60°C in the presence of (b) 0.5, (c) 1, or (d) 1.5 equivalents of Ac_2O . DSs of ca. 2.5, 2.9, and 3 were obtained from the integrals of peaks assigned to protons of the acetyl group (CH_3) and the anhydroglucose unit (AGU)—e.g., $DS = 7 \times I_{(\text{CH}_3, \text{H})} / 3 \times I_{(\text{AGU}, \text{H})}$, where 7 and 3 come from the number of protons in the AGU and the number of hydroxyl groups per AGU. All ^1H NMR spectra were performed at 25°C .

3. Experimental Part

3.1. Materials and Methods

1-Ethyl-3-methylimidazolium chloride (EMIMCl) was purchased from Merck (Saint Louis, MO, USA). Acetic acid (AcOH), acetic anhydride (Ac_2O), microcrystalline cellulose, and Amberlyst were purchased from Sigma-Aldrich (Saint Louis, MO, USA). Ultra-pure water with $18.2\text{ M}\Omega$ of resistivity was obtained from an ELGA Maxima Ultra-Pure Water system (ELGA Berkefeld LabWater, Buckinghamshire, UK). All chemicals were used as received without further purification.

3.2. Transitioning from EMIMCl to EMIMCl·nAcOH upon the Addition of Either AcOH or Ac_2O

EMIMCl·nAcOH-based DESs could be obtained by simple addition of either AcOH or Ac_2O . In the former case, details have been described elsewhere [28]. In the latter case, equimolar amounts of Ac_2O and H_2O (e.g., 0.5, 1, or 1.5 equivalents of Ac_2O and H_2O to obtain DESs with $n = 1, 2$, or 3 , respectively) were added to EMIMCl. EMIMCl·nAcOH-based DESs were obtained after stirring over 6 h, at 60°C .

3.3. Cellulose and EMIMCl Recovery from EMIMCl Solutions of Cellulose Using H₂O as the Antisolvent

EMIMCl solutions of cellulose were prepared by dissolving cellulose either 50 or 200 mg of cellulose in 2.5 g of EMIMCl at 85 °C in 30 min to obtain solution with cellulose contents of 2 and 8 wt%, respectively. Cellulose and EMIMCl recovery using H₂O as the antisolvent was performed by addition of 10 mL of H₂O to the EMIMCl solutions of cellulose at either 20 or 4–5 °C. The mixture was stirred over 2 h at the selected temperature and then centrifuged. The supernatant was a mixture of EMIMCl and H₂O, the freeze-drying of which, and subsequent drying at 60 °C overnight, allowed EMIMCl recovery. The precipitate was cellulose with some remaining EMIMCl that was full recovered after successive washing processes with 10 mL H₂O (up to 4). The washings (e.g., ca. 40 mL) were first freeze-dried, merged with previous fractions of recovered EMIMCl, and then dried at 60 °C overnight for full EMIMCl recovery. The precipitate was also dried at 60 °C for full cellulose recovery.

3.4. Cellulose and EMIMCl Recovery from EMIMCl Solutions of Cellulose Using AcOH as the Antisolvent

For AcOH-assisted cellulose and EMIMCl recovery, AcOH (e.g., either 1–2–3 equivalents, or 10 mL) was added to the EMIMCl solutions of cellulose. The mixtures were stirred at either 20 or 60 °C, over 2 h, and then centrifuged. The supernatant was EMIMCl·*n*AcOH (*n* = 1, 2, 3 or the equivalent to 10 mL, ca. 10), the drying of which at 60 °C overnight provided EMIMCl. The precipitate was cellulose with some remaining EMIMCl·*n*AcOH that was full recovered after successive washing processes with 10 mL H₂O (up to 2). Waters used for washing (e.g., ca. 20 mL) were first freeze-dried, merged with previous fractions of recovered EMIMCl, and then dried at 60 °C overnight for determination of the amount of recovered EMIMCl and characterization. The precipitate was also dried at 60 °C for determination of the amount of recovered cellulose and characterization.

3.5. Cellulose Acetylation in EMIMCl Solutions of Cellulose Using H₂O as the Antisolvent and with the Aid of AcOH as the Acetylating Agent and Amberlyst as the Catalyst

The process was carried out as described above for cellulose recovery using H₂O as the antisolvent and with the aid of AcOH, but in the presence of Amberlyst (e.g., 2 wt%), at 85 °C and stirred over 2 h. The recovered products (e.g., acetylated cellulose and EMIMCl) were dried at 60 °C prior to characterization.

3.6. Cellulose Acetylation in EMIMCl Solutions of Cellulose Using H₂O as the Antisolvent and with the Aid of Ac₂O as the Acetylating Agent

The process was carried out as described above for cellulose recovery using H₂O as the antisolvent, but changing AcOH by equimolar amounts of Ac₂O and H₂O (e.g., either: 0.5 equivalents of Ac₂O and 0.5 equivalents of H₂O instead of 1 equivalent of AcOH; 1 equivalent of Ac₂O, and 1 equivalent of H₂O, instead of 2 equivalents of AcOH; 1.5 equivalents of Ac₂O and 1.5 equivalents of H₂O, instead of 3 equivalents of AcOH). The mixture was stirred at 60 °C, over 2 h. After addition of H₂O (e.g., 10 mL), stirring of the mixture at 60 °C, over 1 h, and subsequent centrifugation, acetylated cellulose was recovered as the precipitate and EMIMCl·*n*AcOH-based DESs (*n* = 1, 2, or 3) were recovered in the supernatant. Full EMIMCl recovery was accomplished by merging of the different fractions obtained after successive washings of acetylated cellulose as described above. The recovered products (e.g., acetylated cellulose and EMIMCl) were dried at 60 °C prior to characterization.

3.7. Sample Characterization

¹H and ¹³C NMR spectra were recorded using a Bruker Avance DRX500 spectrometer (Spectrospin AG, Faellanden, Switzerland) operating at 500 MHz with a 30° pulse, acquisition time of 3.1719 s, relaxation delay of 1 s and 16 scans, and 125.77 MHz, acquisition time of 1.0912 s, relaxation delay of 2 s, and 128 scans, respectively. The samples were

placed in capillary tubes, using deuterated DMSO (DMSO- d_6) as the external reference. Acetylated cellulose samples were dissolved in DMSO- d_6 and placed in 3 mm diameter capillary tubes. The peaks were identified and spectra were processed using the software MestReNova (Mestrelab Research, S.L., Santiago de Compostela, Spain). FTIR spectroscopy was performed with a Bruker IFS66v spectrometer (Karlsruhe, Germany). Raman spectra were recorded with a Renishaw inVia Raman microscope (Old Town Wotton-Under-Edge, Gloucestershire, UK) using irradiation at 514 nm (100% laser power, 2 mW power, 10 accumulations, and an exposure time of 50 s). XRD patterns were obtained on a Bruker D8 Advance diffractometer (Rheinstetten, Germany) using Cu-K α radiation (0.05° step size, 3.5 s counting time). Thermogravimetric analyses (TGAs) were carried out in a TA Instrument TGA Q500 (New Castle, Delaware, USA). Samples were placed in an alumina pan in a sealed furnace and heated at 5 °C min⁻¹ from 25 to 350 °C (for EMIMCl-*n*AcOH mixtures) and from 25 to 700 °C (for cellulose) under a N₂ atmosphere.

4. Conclusions

EMIMCl- and EMIMCl·AcOH-based DESs exhibited quite different solvent capabilities for cellulose; that is, cellulose solubility was high in EMIMCl but basically negligible in EMIMCl·AcOH-based DESs. Thus, as compared with processes using bare H₂O as antisolvent, cellulose and EMIMCl recovery from EMIMCl solutions was improved (mainly in terms of shortening the typically tedious washing cycles to obtain high recovery yields) with the aid of AcOH addition and the transition from EMIMCl- to EMIMCl·AcOH-based DESs. Moreover, acetylated cellulose could also be eventually obtained in high yields when, instead of AcOH, Ac₂O (an efficient acetylation agent) was used for transitioning from EMIMCl- to EMIMCl·AcOH-based DESs.

Supplementary Materials: The following supporting information can be downloaded, Figure S1: TGA curves of EMIMCl, AcOH and EMIMCl HOAc-based mixtures; Figure S2: XRD patterns of regenerated cellulose, Figure S3: Raman spectra of regenerated cellulose, Figure S4: FTIR spectra of regenerated cellulose using H₂O or AcOH as antisolvent, Figure S5: TGA curves of regenerated cellulose using H₂O or AcOH as antisolvent, Figure S6: FTIR spectra of regenerated cellulose using AcOH as antisolvent and Amberlyst as catalyst, Figure S7: TGA curves of regenerated cellulose using H₂O or AcOH as antisolvent and Amberlyst as catalyst, Figure S8: ¹³C NMR spectra of cellulose obtained after acetylation. Figure S9: TGA curves of regenerated cellulose using AcOH or Ac₂O as antisolvent, Figure S10: ¹H NMR spectra of EMIMCl recovered after cellulose acetylation

Author Contributions: Conceptualization, M.L.F. and M.C.G.; methodology, H.Z.; validation, A.I. and P.F.S.; formal analysis, H.Z., A.I. and P.F.S.; investigation, H.Z.; writing—original draft preparation, M.L.F., F.d.M. and M.C.G.; writing—review and editing, M.L.F., F.d.M. and M.C.G.; visualization, M.A.R., A.T. and F.R.A.; supervision, M.C.G.; funding acquisition, M.L.F., F.d.M. and M.C.G. All authors have read and agreed to the published version of the manuscript.

Funding: This research was funded by MINECO/FEDER grant number: RTI2018-097728-B-I00. H. Zhang acknowledges the China Scholarship Council for a PhD research fellowship (CSC No. 201706460015). P.F.-S acknowledges PTI TransEner+ initiative for a research contract.

Institutional Review Board Statement: Not applicable.

Informed Consent Statement: Not applicable.

Data Availability Statement: Not applicable.

Acknowledgments: This work was supported by MINECO/FEDER (Project Number RTI2018-097728-B-I00). H. Zhang acknowledges the China Scholarship Council for a PhD research fellowship (CSC No. 201706460015). The Servicio Interdepartamental de Investigación (SIDI) of the Universidad Autónoma de Madrid is acknowledged for helpful assistance with NMR and DSC studies. P. Carrero at the Instituto de Cerámica y Vidrio (ICV-CSIC) is also acknowledged for help with TGA studies.

Conflicts of Interest: The authors declare no conflict of interest.

Sample Availability: Samples of all the compounds described in this work are available from the authors.

References

1. Wilkes, J.S. A short history of ionic liquids—From molten salts to neoteric solvents. *Green Chem.* **2002**, *4*, 73–80. [[CrossRef](#)]
2. Chatel, G.; Pereira, J.F.B.; Debbeti, V.; Wang, H.; Rogers, R.D. Mixing ionic liquids—“simple mixtures” or “double salts”? *Green Chem.* **2014**, *16*, 2051–2083. [[CrossRef](#)]
3. Abbott, A.P.; Capper, G.; Davies, D.L.; Rasheed, R.K.; Tambyrajah, V. Novel solvent properties of choline chloride/urea mixtures. *Chem. Commun.* **2003**, 70–71. [[CrossRef](#)]
4. Kelley, S.P.; Narita, A.; Holbrey, J.D.; Green, K.D.; Reichert, W.M.; Rogers, R.D. Understanding the Effects of Ionicity in Salts, Solvates, Co-Crystals, Ionic Co-Crystals, and Ionic Liquids, Rather than Nomenclature, Is Critical to Understanding Their Behavior. *Cryst. Growth Des.* **2013**, *13*, 965–975. [[CrossRef](#)]
5. Skarmoutsos, I.; Dellis, D.; Matthews, R.P.; Welton, T.; Hunt, P.A. Hydrogen Bonding in 1-Butyl- and 1-Ethyl-3-methylimidazolium Chloride Ionic Liquids. *J. Phys. Chem. B* **2012**, *116*, 4921–4933. [[CrossRef](#)]
6. Wulf, A.; Fumino, K.; Ludwig, R. Spectroscopic Evidence for an Enhanced Anion–Cation Interaction from Hydrogen Bonding in Pure Imidazolium Ionic Liquids. *Angew. Chem. Int. Ed.* **2010**, *49*, 449–453. [[CrossRef](#)]
7. Seddon, K.R.; Stark, A.; Torres, M.J. Influence of chloride, water, and organic solvents on the physical properties of ionic liquids. *Pure Appl. Chem.* **2000**, *72*, 2275–2287. [[CrossRef](#)]
8. Yasaka, Y.; Wakai, C.; Matubayasi, N.; Nakahara, M. Slowdown of H/D exchange reaction rate and water dynamics in ionic liquids: Deactivation of solitary water solvated by small anions in 1-butyl-3-methylimidazolium chloride. *J. Phys. Chem. A* **2007**, *111*, 541–543. [[CrossRef](#)]
9. Hayes, R.; Imberti, S.; Warr, G.G.; Atkin, R. How Water Dissolves in Protic Ionic Liquids. *Angew. Chem. Int. Ed. Engl.* **2012**, *51*, 7468–7471. [[CrossRef](#)]
10. Mele, A.; Tran, C.D.; De Paoli Lacerda, S.H. The structure of a room-temperature ionic liquid with and without trace amounts of water: The role of C-H...O and C-H...F interactions in 1-n-butyl-3-methylimidazolium tetrafluoroborate. *Angew. Chem. Int. Ed.* **2003**, *42*, 4364–4366. [[CrossRef](#)]
11. Hammond, O.S.; Bowron, D.T.; Edler, K.J. Liquid Structure of the Choline Chloride-Urea Deep Eutectics Solvent (Reline) from Neutron Diffraction and Atomistic Modeling. *Green Chem.* **2016**, *18*, 2736–2744. [[CrossRef](#)]
12. Hammond, O.S.; Bowron, D.T.; Edler, K.J. The Effect of Water upon Deep Eutectic Solvent Nanostructure: An Unusual Transition from Ionic Mixture to Aqueous Solution. *Angew. Chem. Int. Ed.* **2017**, *56*, 9782–9785. [[CrossRef](#)]
13. Hammond, O.S.; Bowron, D.T.; Jackson, A.J.; Arnold, T.; Sanchez-Fernandez, A.; Tsapatsaris, N.; García Sakai, V.; Edler, K.J. Resilience of Malic Acid Natural Deep Eutectic Solvent Nanostructure to Solidification and Hydration. *J. Phys. Chem. B* **2017**, *121*, 7473–7483. [[CrossRef](#)]
14. López-Salas, N.; Vicent-Luna, J.M.; Imberti, S.; Posada, E.; Roldán-Ruiz, M.J.; Anta, J.A.; Balestra, S.R.E.G.; Madero Castro, R.M.; Calero, S.; Riobóo, R.J.; et al. Looking at the “Water-in-Deep-Eutectic-Solvent” System: A Dilution Range for High Performance Eutectics. *ACS Sustain. Chem. Eng.* **2019**, *7*, 17565–17573. [[CrossRef](#)]
15. López-Salas, N.; Vicent-Luna, J.M.; Posada, E.; Imberti, S.; Madero Castro, R.M.; Calero, S.; Ania, C.O.; Riobóo, R.J.; Gutiérrez, M.C.; Ferrer, M.L.; et al. Further Extending the Dilution Range of the “Solvent-in-DES” Regime upon the Replacement of Water by an Organic Solvent with Hydrogen Bond Capabilities. *ACS Sustain. Chem. Eng.* **2020**, *8*, 12120–12131. [[CrossRef](#)]
16. Marcus, Y. Unconventional Deep Eutectic Solvents: Aqueous Salt Hydrates. *ACS Sustain. Chem. Eng.* **2017**, *5*, 11780–11787. [[CrossRef](#)]
17. Zhao, T.; Liang, J.; Zhang, Y.; Wu, Y.; Hu, X. Unexpectedly efficient SO₂ capture and conversion to sulfur in novel imidazole-based deep eutectic solvents. *Chem. Commun.* **2018**, *54*, 8964–8967. [[CrossRef](#)] [[PubMed](#)]
18. Yang, D.; Zhang, S.; Jiang, D. Efficient Absorption of SO₂ by Deep Eutectic Solvents Formed by Biobased Aprotic Organic Compound Succinonitrile and 1-Ethyl-3-methylimidazolium Chloride. *ACS Sustain. Chem. Eng.* **2019**, *7*, 9086–9091. [[CrossRef](#)]
19. Yang, X.; Zhang, Y.; Liu, F.; Chen, P.; Zhao, T.; Wu, Y. Deep eutectic solvents consisting of EmimCl and amides: Highly efficient SO₂ absorption and conversion. *Sep. Purif. Technol.* **2020**, *250*, 117273. [[CrossRef](#)]
20. Yang, D.; Zhang, S.; Jiang, D.; Dai, S. SO₂ absorption in EmimCl–TEG deep eutectic solvents. *Phys. Chem. Chem. Phys.* **2018**, *20*, 15168–15173. [[CrossRef](#)]
21. Yang, D.; Han, Y.; Qi, H.; Wang, Y.; Dai, S. Efficient Absorption of SO₂ by EmimCl–EG Deep Eutectic Solvents. *ACS Sustain. Chem. Eng.* **2017**, *5*, 6382–6386. [[CrossRef](#)]
22. Long, G.; Yang, C.; Yang, X.; Zhao, T.; Xu, M. Deep eutectic solvents consisting of 1-ethyl-3-methylimidazolium chloride and glycerol derivatives for highly efficient and reversible SO₂ capture. *J. Mol. Liq.* **2020**, *302*, 112538. [[CrossRef](#)]
23. Li, Z.-L.; Zhou, L.-S.; Wei, Y.-H.; Peng, H.-L.; Huang, K. Highly Efficient, Reversible, and Selective Absorption of SO₂ in 1-Ethyl-3-methylimidazolium Chloride Plus Imidazole Deep Eutectic Solvents. *Ind. Eng. Chem. Res.* **2020**, *59*, 13696–13705. [[CrossRef](#)]

24. Long, G.; Yang, C.; Yang, X.; Zhao, T.; Liu, F.; Cao, J. Bisazole-Based Deep Eutectic Solvents for Efficient SO₂ Absorption and Conversion without Any Additives. *ACS Sustain. Chem. Eng.* **2020**, *8*, 2608–2613. [[CrossRef](#)]
25. Jiang, W.-J.; Zhang, J.-B.; Zou, Y.-T.; Peng, H.-L.; Huang, K. Manufacturing Acidities of Hydrogen-Bond Donors in Deep Eutectic Solvents for Effective and Reversible NH₃ Capture. *ACS Sustain. Chem. Eng.* **2020**, *8*, 13408–13417. [[CrossRef](#)]
26. Sheng, K.; Kang, Y.; Li, J.; Xu, H.; Li, D. High-Efficiency Absorption of SO₂ by a New Type of Deep Eutectic Solvents. *Energy Fuels* **2020**, *34*, 3440–3448. [[CrossRef](#)]
27. Cao, L.; Huang, J.; Zhang, X.; Zhang, S.; Gao, J.; Zenga, S. High-Efficiency Absorption of SO₂ by a New Type of Deep Eutectic Solvents. *Phys. Chem. Chem. Phys.* **2015**, *17*, 27306–27316. [[CrossRef](#)] [[PubMed](#)]
28. Zhang, H.; Vicent-Luna, J.M.; Tao, X.; Calero, S.; Jiménez-Riobóo, R.J.; Ferrer, M.L.; del Monte, F.; Gutiérrez, M.C. Transitioning from ionic liquids to deep eutectic solvents. *ACS Sustain. Chem. Eng.* **2022**, *10*, 1232–1245. [[CrossRef](#)]
29. Brehm, M.; Pulst, M.; Kressler, J.; Sebastiani, D. Triazolium-Based Ionic Liquids: A Novel Class of Cellulose Solvents. *J. Phys. Chem. B* **2019**, *123*, 3994–4003. [[CrossRef](#)]
30. Brehm, M.; Radicke, J.; Pulst, M.; Shaabani, F.; Sebastiani, D.; Kressler, J. Dissolving Cellulose in 1,2,3-Triazolium- and Imidazolium-Based Ionic Liquids with Aromatic Anions. *Molecules* **2020**, *25*, 3539. [[CrossRef](#)]
31. Vitz, J.; Erdmenger, T.; Haensch, C.; Schubert, U.S. Extended dissolution studies of cellulose in imidazolium based ionic liquids. *Green Chem.* **2009**, *11*, 417–424. [[CrossRef](#)]
32. Uto, T.; Yamamoto, K.; Kadokawa, J. Cellulose Crystal Dissolution in Imidazolium-Based Ionic Liquids: A Theoretical Study. *J. Phys. Chem. B* **2018**, *122*, 258–266. [[CrossRef](#)] [[PubMed](#)]
33. Swatloski, R.P.; Spear, S.K.; Holbrey, J.D.; Rogers, R.D. Dissolution of Cellulose with Ionic Liquids. *J. Am. Chem. Soc.* **2002**, *124*, 4974–4975. [[CrossRef](#)] [[PubMed](#)]
34. Zhu, S.D.; Wu, Y.X.; Chen, Q.M.; Yu, Z.N.; Wang, C.W.; Jin, S.W.; Ding, Y.G.; Wu, G. Dissolution of cellulose with ionic liquids and its application: A mini-review. *Green Chem.* **2006**, *8*, 325–327. [[CrossRef](#)]
35. Swatloski, R.P.; Spear, S.K.; Holbrey, J.D.; Rogers, R.D. Ionic liquid processing of cellulose. *Chem. Soc. Rev.* **2012**, *41*, 1519–1537. [[CrossRef](#)]
36. Sun, N.; Rahman, M.; Qin, Y.; Maxim, M.L.; Rodriguez, H.; Rogers, R.D. Complete Dissolution and Partial Delignification of Wood in the Ionic Liquid 1-Ethyl-3-Methylimidazolium Acetate. *Green Chem.* **2009**, *11*, 646–655. [[CrossRef](#)]
37. Zhang, J.; Zhang, H.; Wu, J.; Zhang, J.; Hea, J.; Xiang, J. NMR spectroscopic studies of cellobiose solvation in EmimAc aimed to understand the dissolution mechanism of cellulose in ionic liquids. *Phys. Chem. Chem. Phys.* **2010**, *12*, 1941–1947. [[CrossRef](#)]
38. Heinze, T.; Schwikal, K.; Barthel, S. Ionic Liquids as Reaction Medium in Cellulose Functionalization. *Macromol. Biosci.* **2005**, *5*, 520–525. [[CrossRef](#)]
39. Bodachivskiy, I.; Page, C.J.; Kuzhiumparambil, U.; Hinkley, S.F.R.; Sims, I.M.; Williams, D.B.G. Dissolution of Cellulose: Are Ionic Liquids Innocent or Noninnocent Solvents? *ACS Sustain. Chem. Eng.* **2020**, *8*, 10142–10150. [[CrossRef](#)]
40. Medronho, B.; Lindman, B. Brief overview on cellulose dissolution/regeneration interactions and mechanisms. *Adv. Colloid Interface Sci.* **2015**, *222*, 502–508. [[CrossRef](#)]
41. Wan, Y.; An, F.; Zhou, P.; Li, Y.; Liu, Y.; Lu, C.; Chen, H. Regenerated cellulose I from LiCl·DMAc solution. *Chem. Commun.* **2017**, *53*, 3595–3597. [[CrossRef](#)] [[PubMed](#)]
42. Makarem, M.; Lee, C.M.; Kafle, K.; Huang, S.; Chae, I.; Yang, H.; Kubicki, J.D.; Kim, S.H. Probing cellulose structures with vibrational spectroscopy. *Cellulose* **2019**, *26*, 35–79. [[CrossRef](#)]
43. Agarwal, U.P.; Reiner, R.S.; Ralph, S.A. Cellulose I crystallinity determination using FT-Raman spectroscopy: Univariate and multivariate methods. *Cellulose* **2010**, *17*, 721–733. [[CrossRef](#)]
44. Liu, C.F.; Sun, R.C.; Zhang, A.P.; Ren, J.L. Preparation of sugarcane bagasse cellulosic phthalate using an ionic liquid as reaction medium. *Carbohydr. Polym.* **2007**, *68*, 17–25. [[CrossRef](#)]
45. Wu, L.M.; Tong, D.S.; Zhao, L.Z.; Yu, W.H.; Zhou, C.H.; Wang, H. Fourier transform infrared spectroscopy analysis for hydrothermal transformation of microcrystalline cellulose on montmorillonite. *Appl. Clay Sci.* **2014**, *95*, 74–82. [[CrossRef](#)]
46. Wu, J.; Zhang, J.; Zhang, H.; He, J.; Ren, Q.; Guo, M. Homogeneous Acetylation of Cellulose in a New Ionic Liquid. *Biomacromolecules* **2004**, *5*, 266–268. [[CrossRef](#)]
47. Wang, H.; Wen, X.; Zhang, X.; Liu, C. Acetylation of Microcrystalline Cellulose by Transesterification in AmimCl/DMSO Cosolvent System. *Molecules* **2017**, *22*, 1419. [[CrossRef](#)]
48. Zweckmair, T.; Hettegger, H.; Abushammala, H.; Bacher, M.; Potthast, A.; Laborie, M.-P.; Rosenau, T. On the mechanism of the unwanted acetylation of polysaccharides by 1,3-dialkylimidazolium acetate ionic liquids: Part 1—Analysis, acetylating agent, influence of water, and mechanistic considerations. *Cellulose* **2015**, *22*, 3583–3596. [[CrossRef](#)]
49. Chen, M.; Li, R.-M.; Runge, T.; Feng, J.; Feng, J.; Hu, S.; Shi, Q.-S. Solvent-Free Acetylation of Cellulose by 1-Ethyl-3-methylimidazolium Acetate-Catalyzed Transesterification. *ACS Sustain. Chem. Eng.* **2019**, *7*, 16971–16978. [[CrossRef](#)]
50. Suzuki, S.; Yada, R.; Hamano, Y.; Wada, N.; Takahashi, K. Green Synthesis and Fractionation of Cellulose Acetate by Controlling the Reactivity of Polysaccharides in Sugarcane Bagasse. *ACS Sustain. Chem. Eng.* **2020**, *8*, 9002–9008. [[CrossRef](#)]
51. Shi, J.; Stein, J.; Kabasci, S.; Pang, H. Purification of EMIMOAc Used in the Acetylation of Lignocellulose. *J. Chem. Eng. Data* **2013**, *58*, 197–202. [[CrossRef](#)]
52. Barthel, S.; Heinze, T. Acylation and carbanilation of cellulose in ionic liquids. *Green Chem.* **2006**, *8*, 301–306. [[CrossRef](#)]

53. Lopes, J.M.; Bermejo, M.D.; Pérez, E.; Martín, Á.; Puras, J.J.S.; Cocero, M.J. Effect of scCO₂ on the kinetics of acetylation of cellulose using 1-allyl-3-methylimidazolium chloride as solvent. Experimental study and modeling. *J. Supercrit. Fluids* **2018**, *141*, 97–103. [[CrossRef](#)]
54. Sun, X.; Lu, C.; Zhang, W.; Tian, D.; Zhang, X. Acetone-soluble cellulose acetate extracted from waste blended fabrics via ionic liquid catalyzed acetylation. *Carbohydr. Polym.* **2013**, *98*, 405–411. [[CrossRef](#)] [[PubMed](#)]